JOURNAL OF APPLIED PHYSICS **114**, 233105 (2013)

Terahertz and direct current losses and the origin of non-Drude terahertz conductivity in the crystalline states of phase change materials

Koichi Shimakawa,[1,2] Tomas Wagner,[1] Miloslav Frumar,[1] Filip Kadlec,[3] Christelle Kadlec,[3] and Safa Kasap[4]

[1]*Department of General and Inorganic Chemistry, University of Pardubice, Pardubice, Czech Republic*
[2]*Department of Electrical Engineering, Gifu University, Japan*
[3]*Institute of Physics, Academy of Sciences of the Czech Republic, Prague, Czech Republic*
[4]*Department of Electrical Engineering, University of Saskatchewan, Saskatoon SK S7N 5A9, Canada*

(Received 27 October 2013; accepted 25 November 2013; published online 19 December 2013)

THz and DC losses in crystalline states of GeSbTe and AgInSbTe phase-change material systems are re-examined and discussed. Although a simple free carrier transport has been assumed so far in the GeSbTe (GST) system, it is shown through recent experimental results that a series sequence of intragrain and intergrain (tunneling) transport, as recently formulated in Shimakawa *et al.*, "The origin of non-Drude terahertz conductivity in nanomaterials," Appl. Phys. Lett. **100**, 132102 (2012) may dominate the electronic transport in the commercially utilized GST system, producing a non-Drude THz conductivity. The extracted physical parameters such as the free-carrier density and mobility are significantly different from those obtained from the Drude law. These physical parameters are consistent with those obtained from the DC loss data, and provide further support for the model. Negative temperature coefficient of resistivity is found even in the metallic state, similar to amorphous metals, when the mean free path is short. It is shown that the concept of *minimum metallic conductivity*, often used in the metal-insulator transition, cannot be applied to electronic transport in these materials. © *2013 AIP Publishing LLC*. [http://dx.doi.org/10.1063/1.4847395]

I. INTRODUCTION

Phase-change materials (PCMs) based on the GeSbTe (called GST) system are well known for their use in rewritable optical data storage devices; commercially realized as DVDs.[1–3] DVDs use the phase change that occurs between the amorphous and crystalline states initiated by focused short laser pulses. The optical and electrical properties of the two phases differ so significantly that this difference is used to store information. A marked contrast of electrical resistivity between the two phases of GeSbTe can be also used for *electrical* data storage, e.g., as in PC random-access memory (PCRAMs) devices.[1] The GST material system has therefore attracted much scientific attention, especially recently, with significant work reporting a number of marked scientific advances in this field (see, for example, Refs. 4–12). A proper description of the charge transport mechanism, particularly in the crystalline state, would therefore be highly useful in further understanding the physics of this phase change material system.

The interaction of THz radiation with charge carriers provides important information on carrier transport in a wide range of materials.[13–17] When the free-carrier scattering time lies around 10^{-13}–10^{-14} s, the most prominent changes in the frequency dependent conductivity is expected to be in the THz energy range. If the medium is homogeneous, free carriers are expected to follow the Drude law. In most electronically conductive nanomaterials, however, deviation from the simple Drude behavior of free carriers within or near the THz range is observed; good recent examples are Refs. 18 and 19, and references therein. One of the most accepted models for the non-Drude behavior was given by Smith[20] and was called the generalized Drude model (or Drude-Smith model). By assuming only one backscattering of free carriers, the real part of conductivity shows a Lorentz-like peak. There is no satisfactory argument that supports the predominance of backscattering only once. The main drawback of the Drude-Smith model is therefore attributed to the lack of a proper physical basis, while the fitting of the model to the experimental data in terms of a phenomenological description is considered to be good as in the examples in Refs. 18 and 19.

Recently, to seek a proper physical origin, an alternative model for the complex conductivity near THz frequencies in nanomaterials has been proposed, in which a series sequence of free (inside the grains, *intragrain*) and tunneling (through grain boundaries, *intergrain*) are taken into account.[21] At higher frequencies, due to the short duration of acceleration time, the free carriers reside inside the grains and hence transport can be simply described by the Drude model. At low frequencies, carriers should pass (tunnel) through grain boundaries. Thus, overall, carriers should experience both free and tunneling events, which lead to a Lorentz-like loss peak. Hereafter, we call this mechanism a series sequence of free and tunneling carriers (SSFTC).

Recent Monte Carlo simulations calculating the THz conductivity of charge carriers in a material with a periodic nanoscale modulation of the potential have predicted, in addition to the Drude term, also the occurrence of a Lorentz-type resonance.[22] This resonance may be understood as due to oscillating charges trapped in deep potential wells. Whereas the theoretical treatment is very different from the SSFTC model, the features predicted by both approaches are similar. The SSFTC model applies essentially to nanometals

 © 2013 AIP Publishing LLC

and nanosemiconductors; and reasonable physical parameters can be extracted from the fitting of the model to experimental data.[21,23,24] It should be noted that there was no report on THz loss in the GST system, while the optical conductivity (from the reflectance measurements) for crystallized $Ge_2Sb_2Te_5$ (GST225) films was reported to follow the Drude law.[25] Recently, systematic data of THz conductivity in both amorphous and crystalline GSTs and related materials have been presented by Kadlec *et al.*,[26] in which the THz conductivity exhibits Lorentz resonance, which has been attributed to a phonon mode and a loss due to free carriers (the Drude law).

As mentioned already, a Lorentz-type resonance can be also produced by the SSFTC mechanism. It is therefore of interest to re-examine the experimental data of THz loss in GSTs and related materials along the SSFTC model. In the present study, therefore, the validity of extracted physical parameters, such as the number of carriers and scattering time, is discussed together with the dc loss in the crystalline states of these phase change materials. We also re-examine the temperature-dependent resistivity with negative temperature coefficient (temperature coefficient of resistivity TCR < 0)[27] by taking into account the multiple scattering of carriers.[28] The concept of *minimum metallic conductivity* (or maximum metallic resistivity), often used in the case of metal-insulator transition, cannot be applied to the electronic transport in GSTs. It is important to emphasize that the transition to and from the crystalline state is actually transitions between an amorphous and a polycrystalline structure for the GST system.

II. MODELS OF ELECTRONIC TRANSPORT

A. THz loss in nanomaterials in metallic states with grain boundary

We first briefly review the SSFTC formalism. The frequency dependence of the complex conductivity $\sigma_f^*(\omega)$ (optical conductivity at an angular frequency ω) for free carriers is given by the Drude law as

$$\sigma_f^*(\omega) = \sigma(0)\frac{1}{1-i\omega\tau} = \frac{e^2 n\tau}{m^*}\frac{1}{1-i\omega\tau} \equiv \sigma_{fR}(\omega) + i\sigma_{fI}(\omega), \quad (1)$$

where $\sigma(0)$ is the Boltzmann dc conductivity, n is the number of free carriers, m^* is the effective mass, τ is the collision or scattering time, ω is the angular frequency of external excitation, taken to be $\exp(-i\omega t)$, and $\sigma_{fR}(\omega)$ and $\sigma_{fI}(\omega)$ are the real and imaginary parts, respectively. For the tunneling conductivity, we use the so-called Dyre expression which is a useful analysis of tunneling (or hopping) carriers as a first approximation.[29–32] The tunneling conductivity, using the Dyre expression and hopping conductivity combined together, with $\exp(-i\omega t)$ as excitation, can be written as[16,24]

$$\sigma_t^*(\omega) = \sigma_t(0)\frac{-i\omega\tau_t}{\ln(1-i\omega\tau_t)} = \left(\frac{n_t(er_t)^2}{2kT\tau_i}\right)\frac{-i\omega\tau_t}{\ln(1-i\omega\tau_t)}, \quad (2)$$

where $\sigma_t(0)$ is the DC tunneling conductivity, n_t is the number of tunneling carriers which is, in general, not the same as n, r_t is the tunneling distance (distance between grains), τ_t is the tunneling time. The overall, or the *effective*, complex conductivity $\sigma_{\mathrm{eff}}^*(\omega)$ in a simple one dimensional approximation may be written as[33]

$$\frac{1}{\sigma_{\mathrm{eff}}^*(\omega)} = \frac{f}{\sigma_f^*(\omega)} + \frac{1-f}{\sigma_t^*(\omega)}, \quad (3)$$

where f is the so-called *spectral weight* of free carriers; or the fractional contribution to the effective conductivity. To extract the complex conductivity, we use the following relationship between the relative permittivity and conductivity under a time dependence of the form $\exp(-i\omega t)$

$$\sigma^*(\omega) = -i\omega\varepsilon_0\varepsilon^*(\omega), \quad (4)$$

where $\varepsilon^*(\omega) + \varepsilon_\infty = \varepsilon_R(\omega) + i\varepsilon_I(\omega)$, ε_0 is the absolute permittivity, $\varepsilon_R(\omega)$ is the real part, and $\varepsilon_I(\omega)$ is the imaginary part, and ε_∞ is the background dielectric constant.

B. DC loss in the metallic state

When the carrier mean free path is short (approaching the Ioffe-Regel criterion[34]), TCR is often negative (TCR < 0) even in metallic states such as amorphous metals.[28] Disorder, for example, due to impurity doping in semiconductors, leads to short mean free paths and the localization of certain electronic states. Then, the carrier multiple scattering may dominate electronic transport and the Boltzmann conductivity σ_B should be modified as[28]

$$\sigma = \sigma_B g^2\left\{1 - \frac{C}{g^2(k_F l)^2}\left(1 - \frac{l}{L}\right)\right\}, \quad (5)$$

where g ($\sim$0.3) is the disorder-induced factor, C ($\sim$1) is a constant, k_F is the wave vector at the Fermi energy, l is the mean free path, and L is the inelastic diffusion length. Note that Eq. (5) is valid only under the condition that $l \le L$. It is known that if the inelastic scattering is dominated by electron-electron interactions, σ increases with T and if the scattering is by phonons, σ increases as $T^{1/2}$, predicting a negative TCR even in the metallic state.[28] In fact, both temperature dependences on σ have been actually observed in amorphous metals, etc.[35] and is empirically given as

$$\sigma(0) = \alpha + \beta T^{\frac{1}{2}} + \gamma T, \quad (6)$$

where α, β, and γ are constants.

As we already stated, in nanomaterials a series connection of the grain and grainboundary dominates the conductivity (see Eq. (3)) and hence the overall or effective dc conductivity is given by

$$\frac{1}{\sigma_{\mathrm{eff}}(0)} = \frac{f}{\sigma_f(0)} + \frac{1-f}{\sigma_t(0)}. \quad (7)$$

III. THz LOSS

Thin films of amorphous PCMs with thickness about 1 μm were deposited onto Si substrates by dc magnetron

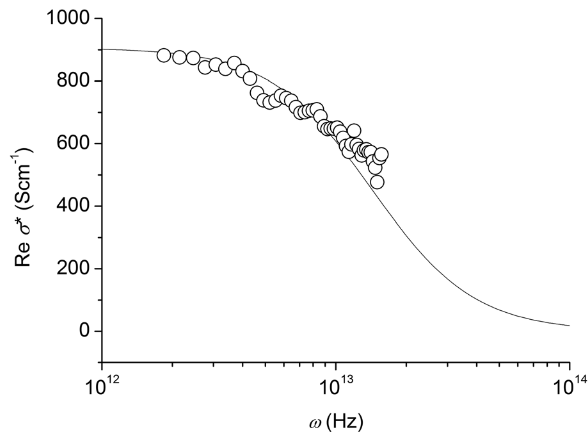

FIG. 1. Experimental (open circle) (data from Ref. 26), and predicted Re $\sigma^*(\omega)$ from the Drude law (solid line) in hexagonal AIST films.

sputtering. PCMs were then annealed at their proper crystallization temperature.[26] The complex refractive index spectra, through the time-domain THz spectroscopy, were determined numerically from the complex transmittance relative to bare Si substrates.[26] As suggested in the previous paper,[21] the imaginary part of the conductivity experimentally deduced is not too reliable and hence we discuss only the real part of the conductivity in the present paper.

We now apply the SSFTC to phase change materials. The discussion will concentrate on *crystalline* PCMs which are prepared by thermal annealing of amorphous PCMs well above their transition temperature. Phonon modes rather than free carriers dominate the THz loss in the amorphous state,[36,37] which is beyond the scope of the present study. Open circles in Fig. 1 show the real part, $\mathrm{Re}\sigma^*(\omega)$, of the THz conductivity (loss) for hexagonal AgInSbTe (AIST) (annealed at 200 °C), which were measured at room temperature.[26] Solid line shows the best fit of the Drude law (Eq. (1)) to the experimental data, with $\sigma(0) = 906\,\mathrm{S\,cm^{-1}}$ and $\tau = 7.0 \times 10^{-14}\,\mathrm{s}$, as summarized in Table I, which are almost the same values as those reported by Kadlec *et al.*[26] Other adjustable parameters are also listed in Table I and these are reasonable. Assuming the effective mass $m^* = 0.3\,m_e$, the free carrier mobility, $\mu = e\tau/m^*$, is estimated to be 410 $\mathrm{cm^2V^{-1}s^{-1}}$, and hence the carrier mean free path $l = \nu\tau \approx 8.4\,\mathrm{nm}$ at 300 K, where the carrier velocity ν is conventionally taken to be the thermal velocity. Clearly, the grain size is expected to be larger than l and hence carriers see a homogeneous medium with less tunneling contribution in the THz frequency range; the result is that, as expected, the transport is simply described by the Drude law for the hexagonal AIST films.

Let us examine the THz loss in the crystalline GST system. While the grain size of the present GST systems are not clear, the size of 5–7 nm[38] and less than 8 nm[39] for GST225 have been reported. Open circles in Figs. 2(a) and 2(b) show the experimental $\mathrm{Re}\sigma^*(\omega)$ for hexagonal (annealed at 300 °C) and distorted rock salt (annealed at 200 °C) GST124, respectively, which were measured at room temperature.[26] The features experimentally observed for GST124 are clearly different from those for AIST. The solid lines in Figs. 2(a) and 2(b) show the best fit of the SSFTC model to the experimental data. The fitting of the model to the experimental data produces the physical parameters that are listed in Table I. Note here that σ_{eff} is $\mathrm{Re}\sigma^*_{\mathrm{eff}}(0)$ and μ_{eff} is given by σ_{eff}/en, which corresponds to so-called Hall mobility.

The present model is comprised of many "free parameters" as shown in Table I. It is possible that the fitting may lead to ambiguous results or interpretation.[23] However, our goal is to seek an understandable physical basis, and one cannot avoid more number of free parameters in the model in as much as we need to consider both *intragrain* and *intergrain* (tunneling) transport in a nanomaterial. Here, the combination of f, n, τ, n_t, and τ_t can be important and if the variables are correctly chosen, the fitting produces reasonable results; that is, values that are physically justifiable.[21]

Next, we discuss the difference of $\mathrm{Re}\sigma^*(\omega)$ between AIST and GST124. A remarkable point is as follows. While the ratio of tunneling contribution, $1-f$, is very small (see Table I), behavior of $\mathrm{Re}\sigma^*(\omega)$ for both hexagonal and distorted rock salt GST124 are drastically changed from free-carrier behavior as observed in AIST. The density of carriers, 1×10^{20} and $5 \times 10^{19}\,\mathrm{cm^{-3}}$, respectively, estimated for both hexagonal and distorted rock salt GST124, are larger than

TABLE I. Physical parameters used for the model calculations in phase change materials. To calculate mobility μ, $m^*/m_e = 0.3$ is assumed for all materials. μ_{eff} ($= \sigma_{\mathrm{eff}}/n$) should correspond to so-called Hall mobility. hex; hexagonal, rock; distorted rock salt, rhom; rhombohedral.

	AIST	GST124		GST112		GeTe
	hex	hex	rock	hex	rock	rhom
f	1.0	0.995	0.95	0.997	0.996	0.995
n (cm^{-3})	1.4×10^{19}	1.0×10^{20}	5.0×10^{19}	2.0×10^{20}	1.0×10^{20}	9.5×10^{19}
τ (s)	7.0×10^{-14}	2.5×10^{-14}	2.0×10^{-14}	2.0×10^{-14}	5.2×10^{-14}	4.3×10^{-14}
μ (cm^{2}V^{-1}s^{-1})	410	150	120	470	310	250
l (nm)	8.4	3.0	1.8	4.2	6.3	5.2
$\sigma(0)$ (Scm^{-1})	910	2300	940	3800	4900	3800
n_t (cm^{-3})	…	9.0×10^{19}	3.5×10^{19}	3.0×10^{19}	1.0×10^{19}	5.0×10^{19}
τ_t (s)	…	9.0×10^{-13}	2.0×10^{-12}	9.0×10^{-13}	1.0×10^{-12}	5.0×10^{-13}
$\sigma_t(0)$ (Scm^{-1})	…	2.0	0.02	1.4	0.3	8.9
σ_{eff} (Scm^{-1})	…	340	1.8	410	76	1200
μ_{eff} (cm^{2}V^{-1}s^{-1})	…	21	0.2	13	4.8	80
r_t (nm)	…	0.8	1.8	1.2	1.0	1.7

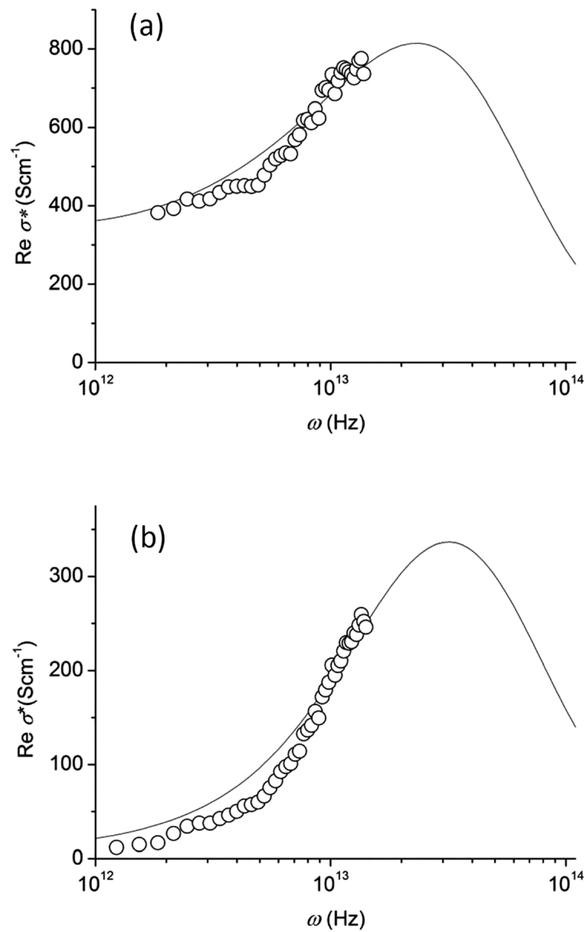

FIG. 2. (a) Experimental (open circle) (data from Ref. 26) and predicted Re $\sigma^*(\omega)$ from the SSFTC model (solid line) in hexagonal GST124 films, and (b) experimental (open circle) (data from Ref. 19), and predicted Re $\sigma^*(\omega)$ from the SSFTC model (solid line) in rhombohedral GST124 films.

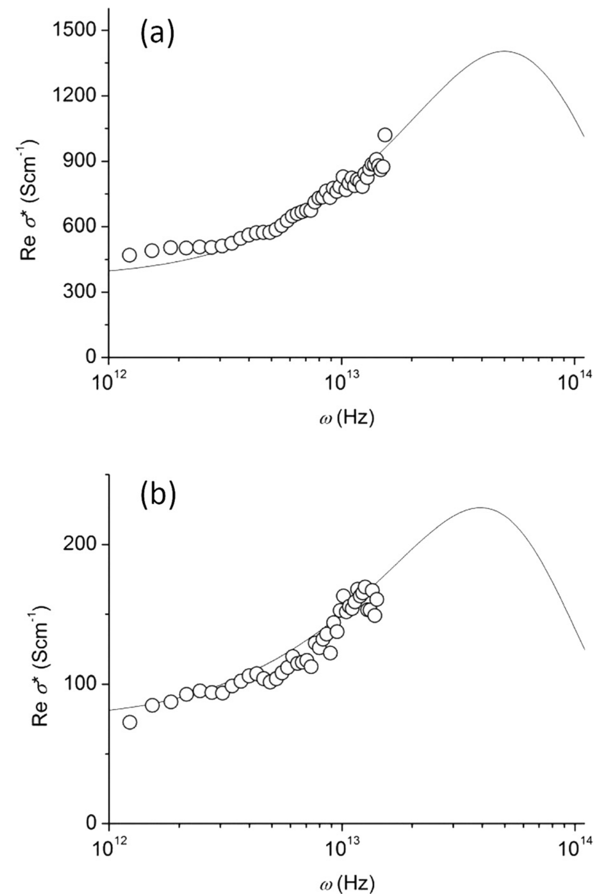

FIG. 3. (a) Experimental (open circle) (data from Ref. 26), and predicted Re $\sigma^*(\omega)$ from the SSFTC model (solid line) in hexagonal GST112 films, (b) experimental (open circle) (data from Ref. 26), and predicted Re $\sigma^*(\omega)$ from the SSFTC model (solid line) in rhombohedral GST112 films.

that ($1.3 \times 10^{19}\,\mathrm{cm}^{-3}$) for AIST. As the fitted carrier scattering time for GST124 is shorter than that for AIST, the resulting free carrier mobility is smaller in GST124 than that in AIST. Both the grain size and the spectral weight f strongly influence the overall features of THz conductivity. It should be noted that due to the tunneling contribution, the overall DC conductivity σ_{eff} and mobility μ_{eff} are almost one or two order of magnitude smaller than those from free carrier contributions, $\sigma_f(0)$ and μ_f. Note also that grain boundary effect in the GST system was ignored and a very small τ ($\sim 5 \times 10^{-15}$ s) was taken into consideration in the previously reported works,[26,27] which is not consistent with the present results. This matter will be discussed later in more detail, together with the dc conductivity in Sec. IV.

Figures 3(a) and 3(b) show the results for $\mathrm{Re}\sigma^*(\omega)$ in hexagonal (annealed at 370 °C) and distorted rock salt (annealed at 200 °C) GST112, respectively. All notations are the same as Figs. 1 and 2. The overall features in GST112 are similar to those in GST124 (see Fig. 2). As shown in Table I, n for the hexagonal structure obtained at higher annealing temperatures is almost the same as those for other crystals. Note also τ deduced for the hexagonal and distorted rock salt are 2×10^{-14} s and 5.2×10^{-14} s, respectively, which produces a relatively high free-carrier mobility μ_f ($=470\ \mathrm{cm}^2\mathrm{V}^{-1}\mathrm{s}^{-1}$ for hexagonal and $305\ \mathrm{cm}^2\mathrm{V}^{-1}\mathrm{s}^{-1}$ for rock salt) and overall mobility μ_{eff} ($=13\ \mathrm{cm}^2\mathrm{V}^{-1}\mathrm{s}^{-1}$ for hexagonal and $4.8\ \mathrm{cm}^2\mathrm{V}^{-1}\mathrm{s}^{-1}$ for distorted rock salt). The smaller μ_{eff} for distorted rock salt than that for hexagonal can be attributed to the tunneling contribution (grain boundary effect), while the free-carrier mobility for the distorted rock salt is much larger than that for the hexagonal crystal.

The last example of $\mathrm{Re}\sigma^*(\omega)$ is shown for the distorted rock salt GeTe in Fig. 4. Crystalline GeTe is known as the simplest ferroelectric material, with only two atoms per unit cell.[40] In GeTe films, thermal annealing at 250 °C produces the rhombohedral crystalline structure.[26,27] The overall features in Fig. 4, for this material, are also similar to those for other material systems. As the tunneling contribution is not significant in this material, σ_{eff} ($=1220\,\mathrm{S\ cm}^{-1}$) and μ_{eff} ($=80\ \mathrm{cm}^2\mathrm{V}^{-1}\mathrm{s}^{-1}$) are relatively higher than those in other systems, while n takes almost the same value as those in the other systems.

Finally, we need to compare the present results with those extracted physical parameters in previous studies. Kadlec *et al.*[26] suggested that THz loss in crystalline PCMs was attributed to both phonon modes (Lorentz type resonance) and free carriers (Drude relaxation). In this model, the intensity of phonon modes in the crystalline state should be larger by almost one order of magnitude than that in the amorphous state. The reason for this is not clear in GSTs. The carrier scattering time τ was estimated to be around 3×10^{-15} s, which

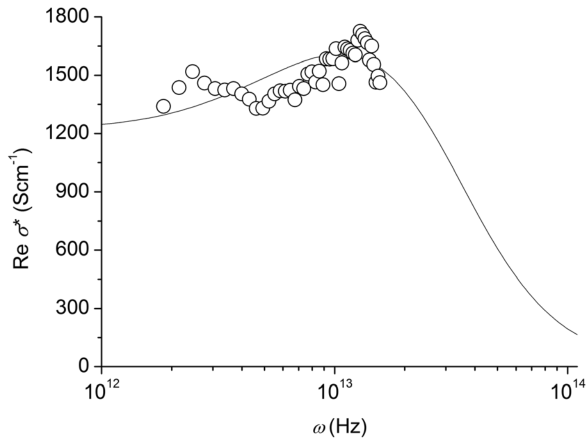

FIG. 4. Experimental (open circle) (data from Ref. 26), and predicted Re $\sigma^*(\omega)$ from the SSFTC model (solid line) in rhombohedral GeTe films.

produces a small mean-free path (<1 nm). As will be discussed below, such a small value leads to the breakdown of the Boltzmann regime. Due to the above reason, we looked for an alternative model to interpret THz conductivity in GSTs and related phase-change materials.

The FTIR and van-der-Pauw experiments on hexagonal GST124 (annealing temperature 300 °C) indicate that $n = 2.2 \times 10^{22}\,\text{cm}^{-3}$, $\tau = 5.1 \times 10^{-15}$ s, $\mu = 23$ $\text{cm}^2\text{V}^{-1}\text{s}^{-1}$ (Hall mobility; μ_{eff} in SSFTC), $\sigma_{\text{vdP}} = 794\,\text{S cm}^{-1}$ (measured DC conductivity; σ_{eff} in SSFTC), carrier mean free path $\lambda_e = 1.75 \times 10^{-7}$ cm (l in SSFTC), and $\sigma_{\text{FTIR}} = 711$ Scm^{-1} ($\sigma(0)$ in SSFTC) are deduced.[27] While some of these, n, μ (so-called Hall mobility), λ_e, and σ_{vdP}, are roughly the same as those in the SSFTC, τ and σ_{FTIR} are different as listed in Table I. It should be mentioned that the FTIR (mid-infrared region) technique applied for GST films might be not sensitive for extracting exact physical parameters related to free-carrier dynamics, as compared with THz spectroscopy.

Let us further examine the physical parameters for distorted rock salt GST124 (annealing temperature 200 °C).[26] Values for n ($= 1.2 \times 10^{20}\,\text{cm}^{-3}$), μ ($= 0.5$ $\text{cm}^2\text{V}^{-1}\text{s}^{-1}$), and $\sigma_{\text{vdP}} = 10$ Scm^{-1}, estimated from the van-der-Pauw method are close to n ($= 5 \times 10^{19}\,\text{cm}^{-3}$), μ_{eff} ($= 0.2$ $\text{cm}^2\text{V}^{-1}\text{s}^{-1}$), and σ_{eff} ($= 1.8\,\text{S cm}^{-1}$) from the SSFTC (see Table I), suggesting that the present model approximately replicates the experimentally obtained transport parameters (van-der-Pauw) as in the hexagonal GST124. The other parameters from the FTIR are very much different from those in SSFTC, e.g., τ ($<0.8 \times 10^{-15}$ s), σ_{FTIR} ($= 52\,\text{S cm}^{-1}$), and $\lambda_e = 0.034$ nm, are very much smaller than those ($\tau = 2 \times 10^{-14}$ s), $\sigma(0)$ ($= 940\,\text{S cm}^{-1}$), and l ($= 1.8$ nm) deduced from the SSFTC. It should be emphasized that such a small value of λ_e (less than lattice constant a) cannot be physically acceptable; i.e., breaking down of the Ioffe-Regel condition ($l \gg a$) and the Boltzmann transport regime (rendering the Hall coefficient itself meaningless).[34] Detailed DC transport mechanisms will be discussed in Sec. IV.

IV. DC LOSS

In a recent paper,[27] a metal-insulator transition through temperature-dependent resistivity measurements (down to 5 K) has been discussed for GST system. The principal results and conclusions are summarized as follows: (i) By changing the annealing temperature, the electronic transport mechanism changes from non-metallic (TCR < 0) to metallic (TCR > 0) at the same critical resistivity (TCR = 0). (ii) A disorder-induced localization produces this critical resistivity of 2–3 mΩ cm, which is often called the *maximum* metallic resistivity (or *minimum* metallic conductivity).

As discussed in Sec. II, negative TCR is also predicted even for the metallic state.[28] A careful discussion on the electronic transport is therefore required for crystalline GSTs, since crystalline GSTs can be a kind of heavily doped metallic semiconductor.[28] Re-examination of the experimental data of the temperature-dependent resistivity is of interest in a region of TCR < 0 by taking into account the multiple scattering of carriers.

Figure 5 shows the temperature-dependent resistivity (5–300 K) in the crystalline states of GST124 annealed at various temperatures (○ at 150 °C, × 175 °C, □ 200 °C, △ 225 °C, ▽ 275 °C). While the resistivity, 2–3 mΩ cm, annealed at 275 °C (▽) is independent of temperature, the others show a resistivity with TCR < 0. Above the annealing at 250 °C, hexagonal GST124 is obtained, in which TCR = 0 and positive TCR are observed.[27] Let us discuss the resistivity with the strongest TCR denoted by open circles (annealed at 150 °C). At this annealing temperature, GST124 may still be a semiconductor in nature (p-type) but E_{F} is very close to the VB and hence we replot the experimental data on conventional ln σ vs. $1/T$ curve as shown in Fig. 6.

As the acceptor energy level is expected to be several meVs, which is due to the high background dielectric constant,[27] the number of free holes should be equal to the number of acceptors at relatively low temperatures (extrinsic region). Therefore, the conductivity (mobility) can be dominated by impurity scattering. Impurity scattering in heavily doped semiconductors dominates the mobility, which is proportional to $T^{2/3}$. The solid line in Fig. 6 shows the $T^{2/3}$ curve, suggesting that the strongest negative TCR originates from impurity scattering. The second term of the right hand in Eq. (7), the tunneling conductivity between grain

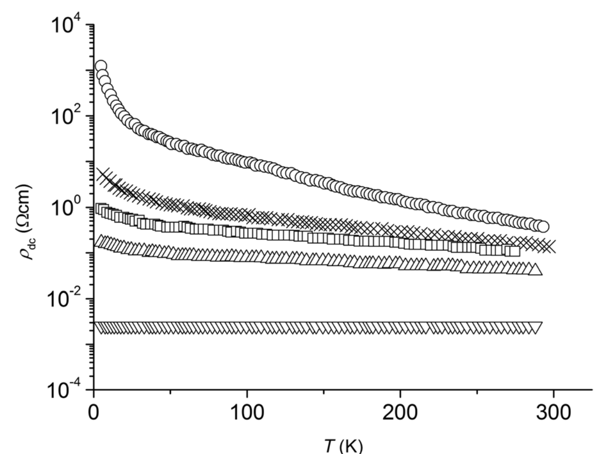

FIG. 5. Resistivity of GST124 films between 5 and 300 K for five samples annealed at 150 °C (○), 175 °C (×), 200 °C (□), 225 °C (△), and 275 °C (▽). Data from Ref. 20.

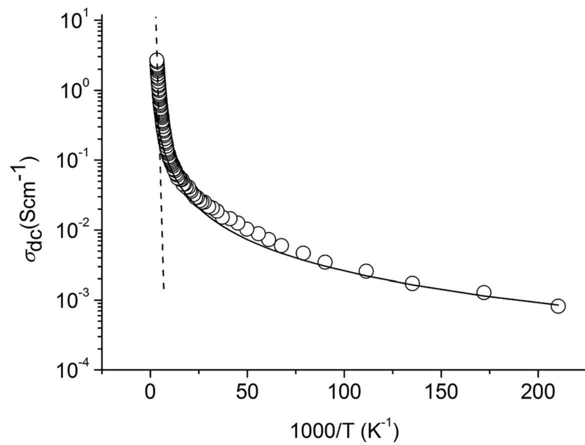

FIG. 6. Temperature dependent conductivity for annealed (150 °C) GST124 films. Open circles are from Ref. 27.

boundaries $\sigma_t(0)$, is ignored ($f/\sigma_f(0) \gg (1-f)/\sigma_t(0)$) due to semiconducting transport in crystalline grains.

At high temperatures, free holes are produced by thermal excitation between bands and hence the conductivity is thermally activated as shown by the dashed line, with an activation energy $\Delta E = 0.16$ eV. Actually, thermally activated electronic transport with an activation energy of 0.14 eV has been reported in rock salt GST225 films.[41] The number of free holes n and the mobility μ at 300 K are deduced to be 1.0×10^{17} cm^{-3} and 164 cm^{2}V^{-1}s^{-1}, respectively, using the relations $n = N_v \exp(-\Delta E/kT)$ with $N_v = 5 \times 10^{19}$ cm^{-3}, and $\sigma = en\mu$. These are very much different from those ($n = 8 \times 10^{19}$ cm^{-3} and $\mu = 0.2$ cm^{2}V^{-1}s^{-1}) reported by Siegrist *et al.*[27] Annealing of GST124 at 150 °C is close to the onset temperature for phase change from amorphous to distorted rock salt structures and hence leads to a large scatter in measurable quantities.

It should be noted that the Mott variable-range-hopping (VRH), i.e., ln ρ vs. $1/T^{1/4}$, was suggested by Siegrist *et al.*,[27] which also fits well to the temperature dependence of resistivity at lower temperatures. At higher temperatures, however, a deviation from VRH is observed and the conductivity is thermally activated as stated above. Hopping of electrons (or holes) between localized states induced by disorder

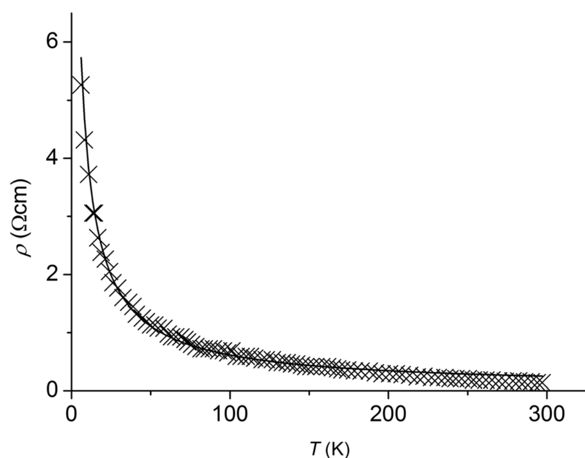

FIG. 7. Temperature dependent resistivity for annealed (175 °C) GST124 films. Crosses are from Ref. 20.

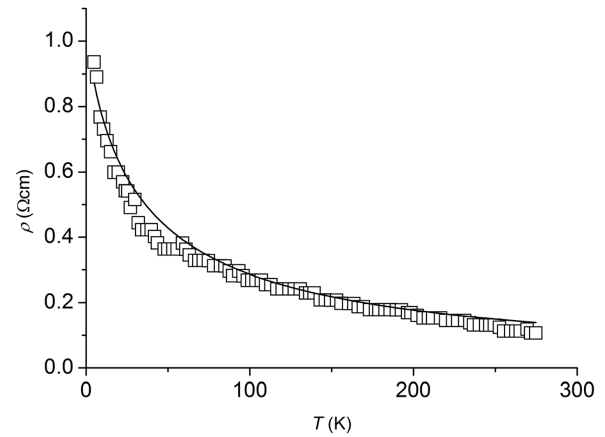

FIG. 8. Temperature dependent resistivity for annealed (200 °C) GST124 films. Squares are from Ref. 27.

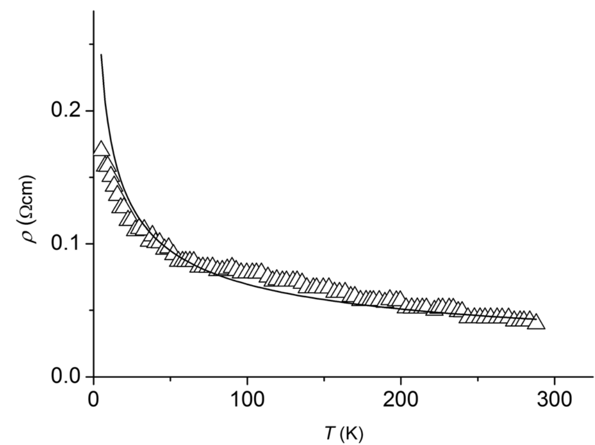

FIG. 9. Temperature dependent resistivity for annealed (225 °C) GST124 films. Triangles are from Ref. 27.

or between acceptors might be the origin of VRH. However, as the extent of localized states (Bohr radius) is expected to be very large (~10 nm) for shallower localized states, a single-phonon process such as VRH, in principle, may not occur in the present materials.[42,43]

Next, temperature-dependent resistivity with weak negative TCR is discussed. Figures 7–9 show ρ vs. T for GST124 annealed at 175 °C (×), 200 °C (□), and 225 °C (△), respectively. For these annealing conditions, the crystalline form of GST124 is distorted rock salt. The fitting of Eqs. (6) and (7) to the experimental results is shown by the solid line in each figure. In each case, the fit is reasonably good; and physical parameters are listed in Table II. The fraction of intragrain transport, f, obtained here from the DC conductivity is very close to that deduced from THz loss. Note also that the

TABLE II. Parameters in Eqs. (6) and (7) for three different annealed GST124. T_a is the annealing temperature.

T_a (°C)	α	β	γ	f	$\sigma_t(0)$ (S cm^{-1})
175	0.04	0.015	0.015	0.95	1.0
200	0.90	0.06	0.02	0.98	3.2
225	1.2	1.1	0.017	0.98	2.0

tunneling conductivity $\sigma_t(0)$ estimated from the DC conductivity here is close to that from THz conductivity (see Tables I and II).

As we discussed in the section on THz loss, the distorted rock salt crystalline GST124 shows the metallic behavior. The DC transport should be also metallic. It is suggested therefore that negative TCR observed for the samples annealed at 175 °C, 200 °C, and 225 °C is metallic in nature, which is usually observed in so-called dirty metals. TCR < 0 or TCR > 0 is not a measure of the metal-insulator transition and there is no minimum metallic conductivity (or maximum resistivity) in the present materials.

V. CONCLUSIONS

It was found that a model involving a series sequence of free (intragrain transport) and tunneling (intergrain transport) carriers, motions describe correctly the non-Drude THz loss in crystalline GSTs. A very small fraction of grain boundary dominates the overall features of electronic transport in crystallized GSTs, which is very different from the previous understanding on GSTs, in which grain boundary effect was completely ignored in discussions. The low carrier mobility experimentally observed in crystalline GSTs can be attributed to the SSFTC mechanism but not due to short scattering time (of the order of femtoseconds) inside the grains. In the present calculations, $\sigma_{\rm eff}$ and $\mu_{\rm eff}$ replicate well the experimentally obtained dc conductivity and Hall mobility, which is a strong point of the present SSFTC model. Within the SSFTC model, the physical parameters deduced from THz spectroscopy are consistent with those extracted from the dc measurements.

It is also suggested that the negative TCR (semiconducting-like property) is observed even for metals with disorder. The concept of *minimum metallic conductivity* (or maximum metallic resistivity), often used in metal-insulator transitions, cannot be applied to the electronic transport in GSTs.

ACKNOWLEDGMENTS

We acknowledge the grant project CZ.1.07/2.3.00/20/0254 *ReAdMat- Research Team for Advanced Non-Crystalline Materials* realized by ESF and Ministry of Education, Youth and Sports of the Czech Republic within ECOP for financial support. F.K. and C.K. acknowledge the funding by the Czech Science Foundation under Grant No. 13-1238ES.

[1]M. Wuttig and N. Yamada, Nature Mater. **6**, 824 (2007).
[2]A. V. Kolobov, P. Fons, J. Tominaga, and T. Uruga, J. Non-Cryst. Solids **352**, 1612 (2006).
[3]N. Yamada, E. Ohno, K. Nishiuchi, N. Akahira, and M. Takao, J. Appl. Phys. **69**, 2849 (1991).
[4]K. Ren, F. Rao, Z. Song, L. Wu, M. Xia, B. Liu, and S. Feng, J. Appl. Phys. **113**, 234312 (2013).
[5]Y. Lu, Z. Zhang, S. Song, X. Shen, G. Wang, L. Cheng, S. Dai, and Z. Song, Appl. Phys. Lett. **102**, 241907 (2013).
[6]Y. Gu, S. Song, Z. Song, S. Bai, Y. Cheng, Z. Zhang, B. Liu, and S. Feng, Appl. Phys. Lett. **102**, 103110 (2013).
[7]G. W. Burr, P. Tchoulfian, T. Topuria, C. Nyffeler, K. Virwani, A. Padilla, R. M. Shelby, M. Eskandari, and B. Jackson, J. Appl. Phys. **111**, 104308 (2012).
[8]A. Gyanathan and Y.-C. Yeo, J. Appl. Phys. **112**, 104504 (2012).
[9]K. Makino, J. Tominaga, A. V. Kolobov, P. Fons, and M. Hase, Appl. Phys. Lett. **101**, 232101 (2012).
[10]J. M. Skelton, D. Loke, T. H. Lee, and S. R. Elliott, J. Appl. Phys. **112**, 064901 (2012).
[11]M. Krbal, A. V. Kolobov, P. Fons, J. Tominaga, S. R. Elliott, J. Hegedus, and T. Uruga, Phys. Rev. B **83**, 054203 (2011).
[12]B. Huang and J. Robertson, Phys. Rev. B **81**, 081204 (2010).
[13]J. Lloyd-Hughes and T.-I. Jeon, J. Infrared Millim. Waves **33**, 871 (2012) provides an extensive review of various models; see references therein.
[14]J. Lloyd-Hughes, Appl. Phys. Lett. **100**, 122103 (2012).
[15]I. H. Baek, K. J. Ahn, B. J. Kang, S. Bae, B. H. Hong, D.-I. Yeom, K. Lee, Y. U. Jeong, and F. Rotermund, Appl. Phys. Lett. **102**, 191109 (2013).
[16]H. Wan, J. Q. Guo, and Y. S. Zhou, Carbon **64**, 67 (2013).
[17]R. A. Lewis, *Terahertz Physics* (Cambridge University Press, Cambridge, New York, 2012).
[18]T. L. Cocker, L. V. Titova, S. Fourmaux, H.-C. Bandulet, D. Brassard, J.-C. Kieffer, M. A. E. Khakani, and F. A. Hegmann, Appl. Phys. Lett. **97**, 221905 (2010).
[19]D. G. Cooke, A. Meldrum, and P. U. Jepsen, Appl. Phys. Lett. **101**, 211107 (2012).
[20]N. V. Smith, Phys. Rev. B **64**, 155106 (2001).
[21]K. Shimakawa, T. Itoh, H. Naito, and S. O. Kasap, Appl. Phys. Lett. **100**, 132102 (2012); 239901 (2012) Erratum; Phys. Status Solidi C **9**, 2602 (2012).
[22]J. Mrozek and H. Němec, Phys. Rev. B **86**, 075308 (2012).
[23]R. Lovrinčic, Appl. Phys. Lett. **102**, 096101 (2013).
[24]K. Shimakawa, T. Itoh, H. Naito, and S. O. Kasap, Appl. Phys. Lett. **102**, 096102 (2013).
[25]A. Mendoza-Galvan and J. Gonzalez-Hernandez, J. Appl. Phys. **87**, 760 (2000).
[26]F. Kadlec, C. Kadlec, and P. Kužel, Solid State Commun. **152**, 852 (2012).
[27]T. Siegrist, P. Jost, H. Volker, M. Woda, P. Merkelbach, C. Schlockermann, and M. Wuttig, Nature Mater. **10**, 202 (2011).
[28]N. F. Mott, *Conduction in Non-Crystalline Materials*, 2nd ed. (Clarendon Press, Oxford, 1993).
[29]J. C. Dyre, Phys. Lett. **108A**, 457 (1985).
[30]J. C. Dyre, J. Appl. Phys. **64**, 2456 (1988).
[31]J. C. Dyre, Phys. Rev. B **48**, 12511 (1993).
[32]J. C. Dyre, Rev. Mod. Phys. **72**, 873 (2000).
[33]See Chapter 2 in *The Springer Handbook of Electronic and Photonics Materials*, edited by S. Kasap and P. Capper (Springer, New York, 2007).
[34]A. F. Ioffe and A. R. Regel, Prog. Semicond. **4**, 237 (1960).
[35]A. Möbius, J. Phys. C **18**, 4639 (1985).
[36]S. N. Taraskin, S. I. Simdyanskin, S. R. Elliott, and T. Lo, Phys. Rev. Lett. **97**, 05504 (2006).
[37]M. Zalkovskij, C. Z. Bisgard, A. Novitsky, R. Malureanu, D. Savastru, A. Popescu, P. U. Jepsen, and A. V. Lavrinenko, Appl. Phys. Lett. **100**, 031901 (2012) .
[38]T. Wagner, J. Orava, J. Prikryl, T. Kohoutek, M. Bartos, and M. Frumar, Thin Sold Films **517**, 4694 (2009).
[39]M. Frumar, T. Wagner, J. Prikryl, J. Orava, and T. Wagner, Phys. Status Solidi B **246**, 1871 (2009).
[40]F. Kadlec, C. Kadalec, P. Kuzel, and J. Petzelt, Phys. Rev. B **84**, 205209 (2011).
[41]T. Kato and K. Tanaka, Jpn. J. Appl. Phys., Part 1 **44**, 7340 (2005).
[42]K. Shimakawa and K. Miyake, Phys. Rev. Lett. **61**, 994 (1988).
[43]K. Shimakawa and K. Miyake, Phys. Rev. B **39**, 7578 (1989).